Title

Physical Modeling of Stone Columns in Unsaturated Soil Deposits

Journal

Geotechnical Testing Journal, 43(1)

ISSN

0149-6115

Authors

Maghvan, Sajjad Vaseghi
Imam, Reza
McCartney, John S

Publication Date

2020

DOI

10.1520/gtj20170405

Peer reviewed

PHYSICAL MODELING OF STONE COLUMNS IN UNSATURATED SOIL DEPOSITS

Journal:	*Geotechnical Testing Journal*
Manuscript ID	GTJ-2017-0405.R3
Manuscript Type:	Technical Manuscript
Date Submitted by the Author:	n/a
Complete List of Authors:	Vaseghi Maghvan, Sajjad; Amirkabir University of Technology, Department of Civil and Environmental Engineering Imam, Reza; Amirkabir University of Technology, Department of Civil and Environmental Engineering McCartney, John; University of California San Diego, Department of Structural Engineering
ASTM Committees and Subcommittees:	D18.05 Strength and Compressibility of Soils < D18 Committee on Soil and Rock
Keywords:	unsaturated soil, bearing capacity, stone column
Abstract:	This paper focuses on evaluating the load-settlement response of circular footings on unsaturated soil layers improved with stone columns using 1-gravity (1g) physical modeling experiments. The initial (pre-loading) conditions in the soil layers were varied by compaction to the same dry density but different initial degrees of saturation. An effective stress analysis calibrated using direct shear experiments was found to satisfactorily predict the measured bearing capacities of unimproved soil layers, considering a change in failure mode for soil specimens at certain initial degrees of saturation. As the bearing capacity of the unsaturated soil layers increased, the amount of improvement gained by incorporating stone columns decreased. Bulging deformations of the stone column exhibited a close relationship with the bearing capacity, with smaller amounts of bulging in soil layers with low initial degrees of saturation that also have high bearing capacity. The stress concentration ratio increases with increasing initial degree of saturation, indicating that stone columns carry a greater fraction of the applied footing stress for soil layers closer to saturated conditions.

PHYSICAL MODELING OF STONE COLUMNS IN UNSATURATED SOIL DEPOSITS

Sajjad Vaseghi Maghvan[1], Reza Imam[2], John S. McCartney[3]

Abstract

This paper focuses on evaluating the load-settlement response of circular footings on unsaturated soil layers improved with stone columns using 1-gravity (1g) physical modeling experiments. The initial (pre-loading) conditions in the soil layers were varied by compaction to the same dry density but different initial degrees of saturation. An effective stress analysis calibrated using direct shear experiments was found to satisfactorily predict the measured bearing capacities of unimproved soil layers, considering a change in failure mode for soil specimens at certain initial degrees of saturation. As the bearing capacity of the unsaturated soil layers increased, the amount of improvement gained by incorporating stone columns decreased. Bulging deformations of the stone column exhibited a close relationship with the bearing capacity, with smaller amounts of bulging in soil layers with low initial degrees of saturation that also have high bearing capacity. The stress concentration ratio increases with increasing initial degree of saturation, indicating that stone columns carry a greater fraction of the applied footing stress for soil layers closer to saturated conditions.

KEWORDS: Unsaturated Soil, Degree of Saturation, Matric Suction, Bearing Capacity, Stone Column, Bulging, Shear Strength.

[1] Lecturer, Amirkabir University of Technology, Dept. of Civil and Environmental Engineering, Tehran, Iran, 0098 91 4530 7488, svmagvan-sf69@aut.ac.ir.

[2] Assistant Professor, Amirkabir University of Technology, Dept. of Civil and Environmental Engineering, Tehran, Iran, 0098 21 6454 3040 (Corresponding Author), rimam@aut.ac.ir.

[3] Professor and Department Chair, University of California San Diego, Dept. of Structural Engineering. 9500 Gilman Dr., La Jolla, CA 92093-0085, mccartney@ucsd.edu.

INTRODUCTION

Over the past four decades, stone columns (also known as granular columns or granular piles) have been among the most extensively used methods of soil improvement. They have been used in a wide variety of soils, ranging from loose sands to soft compressible clays for increasing the bearing capacity and minimizing the settlement of shallow footings (Shivashankar et al., 2010). A topic that has not been fully investigated is the role of unsaturated soil conditions in the improvement of soil layers with stone columns. This is a relevant topic because most of the deformation in a stone column is expected near the ground surface, which is typically unsaturated (Fredlund, 2014). It has been estimated that 40% of the people in the world live in arid areas (Khalili et al., 2000), where stone columns may be an economical method of soil improvement. Changes in the degree of saturation are expected to cause significant changes in the shear strength and shear-induced volume change response of soils (Gens et al., 2006; Imam et al., 2018), altering the interaction between a soil layer and a stone column.

Although stone columns are widely used in geotechnical projects, present design methods are mostly empirical (Ambily and Gandhi, 2007). The unit cell concept is usually used for the purposes of determining the bearing capacity and settlement of a soil layer improved with stone columns (Barksdale and Bachus, 1983). The unit cell refers to the cylindrical unit of the approximately circular area converted from the influence zone of a stone column (Das and Deb, 2016), assuming an infinitely-wide loaded area of soil improved with stone columns having constant diameter and spacing (Shahu and Reddy, 2011). The failure mode for a single stone column in a weak soil layer under surficial compressive footing loads depends on the critical length of the stone column, which ranges from 4 to 6 times the diameter of the column, equal to

the length of the upper portion of the stone column that can bear the ultimate footing load (regardless of the surface settlement) (Hughes and Withers, 1974). Three failure models for single stone columns have been observed: bulging failure (for columns with length greater than critical) (Hughes and Withers, 1974), general shear failure (i.e., for end bearing stone columns with length shorter critical) (Madhav and Vitkar, 1978), and punching failure (i.e., for floating stone columns with length shorter than critical) (Aboshi et al., 1979). A bulging failure mechanism is observed for stone columns with length greater than critical, regardless of its being end bearing or floating (Barksdale and Bachus, 1983; Black et al., 2007). Stone columns with a length greater than critical do not show additional increases in bearing capacity with length, although greater lengths may be needed to reduce the footing settlement (Babu et al., 2013).

Several experimental studies have been performed to understand the degree of improvement associated with improving weak soil layers with stone columns (Ayadat and Hanna, 2005; Ambily and Gandhi, 2007; Deb et al., 2011). Although previous studies have evaluated the improvement of compacted soil layers with stone columns, they have not systematically evaluated the impact of unsaturated conditions on the bearing capacity, settlement, and deformation of stone columns constructed in unsaturated soils. During the last 50 years several studies have been carried out on the investigation of the effect of unsaturated conditions on the bearing capacity of model shallow footing over unsaturated soil layers (Broms, 1965; Steensen-Bach et al., 1987; Fredlund and Rahardjo, 1993; Schnaid et al., 1995; Oloo et al., 1997; Miller and Muraleetharan, 1998; 2003; Costa et al., 2003; Mohamed and Vanapalli, 2006; Oh and Vanapalli, 2011; Vanapalli and Mohamed, 2013; Vahedifard and Robinson, 2015; Tang et al., 2016). However, they did not consider the impact of unsaturated soil conditions on the improvement

gained by including a stone column. Accordingly, the main objective of this study is to investigate the influence of unsaturated conditions on the level of improvement of an unsaturated soil layer due to presence of a single stone column.

EXPERIMENTAL PROGRAM

Testing Plan Overview

Model tests were carried out on a single stone column having a diameter of 50 mm in a square tank. Effects of the degree of saturation of surrounding soils on the bearing capacity and settlement of a footing on surface of soil layers with and without a stone column, as well as on the bulging response of the stone column were investigated. The bearing capacity measurements were made to determine the bearing improvement ratio of the stone column (i.e., the ratio of the bearing capacity of improved to unimproved soil layers).

To allow for application of results from the current study to in-situ soil conditions, several scaling considerations were considered in conducting the model tests. First, the soil particle size was selected such that the ratio of footing width to average soil particle size is greater than 165, the minimum value recommended by previous researchers (e.g., Lau and Bolton, 2011) for the elimination of the effects of grain size on the test results. Second, the sand tested was placed in a relatively loose state (i.e., relative density of 40%) such that the stress-strain response in the lower-stress model tests is similar to the higher-stress in-situ conditions, where soils are typically denser, as suggested in the scaling approach of Iai (1989). Based on the concept of critical state soil mechanics, the behavior of loose sand consolidated to low stress is similar to dense sand consolidated to high stress, since these two conditions result in a similar state parameter. This parameter is defined as the difference in void ratio at the

current state and the critical state at the same mean effective normal stress in a plot of void ratio vs. mean effective normal stress. Validity of this approach was also examined by Cerato and Lutenegger (2007), who measured the load-settlement curve of footings with various dimensions and stress levels and concluded that footings on soil layers having the same state parameter exhibit the same behavior. Scale effect caused by footing size can also be considered by plotting the applied stress versus 'settlement/footing dimension' (i.e., s/D) curves (i.e., normalized settlement) (Palmer, 1948). Third, model footing tests on unsaturated soils should also be interpreted taking into account the matric suction developed in such soils. Foundations often rest on soils above groundwater table, where soil moisture and matric suction vary with depth. In these cases, average matric suction should be used in the calculations of bearing capacity. The average matric suction is a function of the footing dimension; smaller footings would have greater average matric suction than larger footings since the averaged zone is closer to the ground surface, where the degrees of saturation is lower and matric suction is higher. In the current study, a uniform profile of moisture with depth was added to the tested soil in order to simplify the interpretation of the results and avoid the need for averaging matric suctions, which may be influenced by scale effects (Oh and Vanapalli, 2013). It is noted, however, that the effects of scaling relationships on the behavior of unsaturated soil layers is still considered uncertain and is a topic for future research.

Materials

A silty sand known as Firoozkooh 101 sand (FK 101) having the grain size distribution shown in Figure 1(a) was used in this study. The soil is classified as SP-SM according to the Unified Soil Classification Scheme (USCS). The stone column material has a relatively uniform

grain size distribution and particle sizes ranging from 2 mm to 4.75 mm, as shown in Figure 1(a), and is classified as SP according to the USCS. The materials were selected to meet scaling relationships between the model scale and a prototype in the field. The geotechnical properties of the silty sand and stone column material are summarized in Table 1. The contact filter paper method using ash-free, low rate, Whatman No. 42 with a 2.5 μm pore size was employed for the determination of matric suction of the sand to define its water retention curve (SWRC). The SWRC of the sandy soil at a relative density of 40% was obtained using the filter paper calibration curve provided by ASTM D5298 and the data was fitted using the SWRC model of van Genuchten (1980), given as follows:

$$S_e = \left[\frac{1}{1 + \{\alpha_{vG}(u_a - u_w)\}^{n_{vG}}}\right]^{(1 - 1/n_{vG})} \quad (1)$$

where u_a is the pore air pressure, u_w is the pore water pressure, $(u_a - u_w)$ is the matric suction, α_{vG} and n_{vG} are fitting parameters, and S_e is the effective saturation defined as follows:

$$S_e = \frac{S_r - S_{res}}{1 - S_{res}} \quad (2)$$

where S_r is the degree of saturation and S_{res} is the residual saturation. The SWRC data along with the fitted SWRC of van Genuchten (1980) for the sand are shown in Figure 1(b). The air-entry value (AEV) and the residual state of saturation (i.e., S_{res}) and the van Genuchten (1980) SWRC fitting parameters are summarized in Table 1. The degree of saturation is the same as the effective saturation for this soil as the residual saturation is zero for this soil. It is noted that the soil tested is a standard local silty sand prepared by crushing parent rock, and its fines content consists of non-plastic, rock flour. It is common to assume that non-plastic soils will have a zero

residual saturation. The fit shows a zero residual saturation, and the data, albeit with some scatter, support this trend. Brooks and Corey (1964), Clayton (1996), McCartney et al., (2005), and Bouazza et al., (2013) have also obtained a S_{res} of zero or near-zero for sandy soils in their studies.

Direct shear tests were performed on the unsaturated sand specimens at seven different initial (pre-loading) degrees of saturation of 0, 4, 16, 30, 60, 90 and 100% under initial vertical stresses of 50, 100, and 200 kPa. Direct shear tests permit an understanding of the effects of the degree of saturation on both the shear strength and the shape of the stress strain curve, and it is expected that results obtained from tests with other stress paths, such as the triaxial test, will exhibit similar trends. Compaction of the soil at various degrees of saturation may lead to differences in fabric of the compacted soil. However, examination of these effects was not within the scope of this study. Details of the direct shear test results of the soil are provided by Imam et al. (2018). The relationship between the shear strength and initial degree of saturation of the sandy soil compacted to initial relative density of 40% is shown in Figure 2(a). The direct shear tests in this study were interpreted in terms of effective stress, using a form of the effective stress proposed by Lu et al. (2010), given as follows:

$$\sigma' = (\sigma - u_a) - \sigma^s \quad (3)$$

where σ' is the effective stress, σ is the total stress, u_a is the pore air pressure, and σ^s is the suction stress, defined as the product of the effective saturation and the matric suction. This permits the SWRC model in Equation (1) to be integrated into the effective stress, as follows:

$$\sigma' = (\sigma - u_a) + \frac{S_e}{\alpha_{vG}}\left(S_e^{\frac{n_{vG}}{1-n_{vG}}} - 1\right)^{\frac{1}{n_{vG}}} \quad (4)$$

The Mohr-Coulomb failure criterion can be used to predict the impact of effective saturation on the shear strength of unsaturated soils, as follows (Lu et al., 2010):

$$\tau_f = c' + \left[(\sigma - u_a) + \frac{S_e}{\alpha_{vG}}\left(S_e^{\frac{n_{vG}}{1-n_{vG}}} - 1\right)^{\frac{1}{n_{vG}}}\right]\tan\phi' \quad (5)$$

where τ_f is the shear stress at failure at a given effective saturation, c' is the drained cohesion (typically assumed to equal zero for uncemented soils), and ϕ' is the drained friction angle. The internal friction angle is assumed to not vary with the degree of saturation or matric suction (Bouazza et al., 2006; Oh et al., 2011).

The failure envelopes for the unsaturated silty sand at different initial degrees of saturation are shown in Figure 2(b). The drained friction angles and apparent cohesion values along with the coefficients of determination, R^2, for the different failure envelopes are listed in Table 2. The apparent cohesion was determined as the ordinate intercept of the failure envelopes, which were assumed to have the same slope. Experimental values of suction stress can be estimated from the shear strength values τ_f obtained from the failure envelopes in Figure 3(b) and a value of c' equal to zero, as follows (Lu et al., 2010):

$$\sigma^s = -\frac{\tau_f - (\sigma - u_a)\tan\phi'}{\tan\phi'} \quad (6)$$

The suction stress values estimated from the model of Lu et al. (2010) incorporating the parameters of the SWRC in Figure 1(b) along with the suction stress values estimated from the failure envelopes are shown in Figure 2(c). A good match between the predicted and measured

suction stress values is observed, which confirms that an effective stress analysis is appropriate for interpretation of the behavior of stone columns in unsaturated soil layers.

Soil Placement and Stone Column Installation Procedures in the Physical Modeling Tests

To understand the effects of improvement of unsaturated soils layers with stone columns, a physical modeling experimental program was performed in a tank having areal dimensions of 500 mm × 500 mm and a height of 1000 mm. The soil was placed in the tank in 50 mm-thick lifts to reach an initial relative density of 40% in all tests. Before soil placement, the inner walls of the tank were coated with a thin polyethylene sheet to reduce the interface friction between the walls and the soil. The soil was mixed with various percentages of water such that six target degrees of saturation of 0, 4, 16, 30, 60, and 90% at the time of loading could be achieved. Each soil lift was layer compacted using a square hammer, then the final surface was leveled using a trowel. The same method of placement was used for all the tests conducted at various initial degrees of saturation. The soil placed was maintained at an isolated condition by covering the tank with plastic sheets and keeping it at a constant temperature and humidity for 7 days for the degree of saturation to homogenize. Moisture added to the soil at the time of mixing was slightly higher such that the desired initial (pre-loading) degree of saturation just before loading of the circular footing would be achieved. It was noticed that the additional moisture needed to compensate for subsequent losses of moisture and achieve the target initial degrees of saturation was somewhat higher for higher target degrees of saturation. The variations in the soil relative density after compaction for each test were determined using a cylindrical hollow sampling tube and are presented in Figure 3.

After placing the soil layers, an open-ended tube with an outer diameter of 50 mm and a wall-thickness of 2 mm was pushed into the unsaturated soil. Because of the apparent cohesion, the unsaturated soil inside the tube could be extracted from the soil layers without causing significant disturbance. Using the known volume of the hole and considering the target relative density of the stone column material of 60%, the total weight of the stone column material was determined and divided into 9 equal batches, each providing the material needed to construct a 50-mm high section of the stone column. To construct each section of the stone column, the tube was re-inserted into the hole and pulled up in 50 mm increments, after which the stone column material was poured in and compacted until it was at the same level as the lower end of the tube, leading to a 50 mm-thick lift. This approach assumes negligible lateral deformation of the stone column during compaction. This procedure was repeated until the final height of the stone column reached 450mm.

The steps of installation of the stone column in the soil layers are shown in Figure 4.The bottom of the stone column was extended to the bottom of the test tank, which means that the stone column has an end bearing bottom boundary condition. After construction of the stone column, the top of the soil surface and the stone column were carefully leveled and covered with plastic sheets for 7 days to reach hydraulic equilibrium.

Testing Procedures

Tests were performed on the improved and unimproved soil layers by measuring the stress-settlement curve of a circular aluminum footing having a diameter of 100 mm and a thickness of 15 mm located at the surface of the soil layer in the center of container. The footing was loaded in a displacement-controlled manner at a rate of 1 mm/min. The first series was

performed on the footing atop unimproved (i.e., no stone column) soil layers having different initial degrees of saturation. The second series was performed on the footing atop soil layers having the same initial degrees of saturation as the first series but improved with a single stone column in the center of the soil layer to investigate the effects of stone column improvement on the stress-settlement curve and the corresponding deformation of the soil surface and stone column. It was expected that the lateral constraints of the surrounding unsaturated soil layers will contribute to carrying the applied footing stress, enhancing the bearing capacity of the soil layers. The profile of the degrees of saturation at the times of loading for both the unimproved and improved soil layers are presented in Figure 5. The degrees of saturation at the time of loading is the average of the values measured in each test for the soil specimens from the soil surface to a depth of 200 mm, however, as can be noticed from Figure 5, values of the degrees of saturation (and consequently, the soil suctions) were relatively uniform throughout the soil layer height, at least within the depths they were measured. It is expected that the stone column failure and stress-settlement behavior are controlled primarily by the properties of the soil within this depth, which is equivalent to twice the diameter of the loading plate.

To evaluate the soil surface bulging caused by loading the footing caused by loading, the final surface of the soil layers was leveled carefully after compaction, then painted using a color spray paint. This approach also served to help minimize surface evaporation during the footing loading stage when there was no plastic wrap on the soil surface. Knowing the area of the loading plate, the applied average pressure under the loading plate was calculated. Details of the equipment and the accessories used during the loading stage of the tests are shown in Figure 6.

RESULTS

Stress-Settlement Curves for Unimproved Soil Layers

The relationships between the applied footing stresses versus vertical settlement of the shallow footing on unimproved soil layers at different initial degrees of saturation are shown in Figure 7. When the initial degree of saturation increases from 0 to 16%, an increase in bearing capacity is observed. For higher initial degrees of saturation, the bearing capacity decreases. The minimum bearing capacity of the soil is observed for an initial degree of saturation of 90%. It is expected that a saturated soil layer will have an even lower bearing capacity. An issue that must be addressed is that in the degrees of saturation less than 30%, stress- settlement response of the soil has a peak at the settlements corresponding to 10 to 20 mm. However, for the unsaturated soils layers at initial degrees of saturation of 60 and 90%, the bearing capacity increases monotonically with the increase in the footing displacement. The bearing capacity sensitivity to changes in initial degree of saturation is less at high initial degrees of saturation than that at lower initial degrees of saturation.

Surface bulging occurred, and its value increased at footing settlements up to 20 to 30 mm, after which no change was observed in the shape of the surface bulges, and only the depth and width of the cracks increased. The heights of surface bulging of the soil layers having various initial degrees of saturation are summarized in Figure 8. The shape of the surface bulging shown in this figure is pertinent to footing settlement of approximately 20 mm. It is expected that the tested soil at a relative density of 40% will experience local shear failure (Vesić, 1973). For unsaturated soil layers, the degree of saturation seems to influence the failure mechanism of the soil. The failure mode (i.e., general shear, local shear, or punching shear failure) also depends on the size of the footing compared to the particle size of the soil. For a relatively large footing, the

soil matric suction offers more resistance. However, when a footing size is relatively small, the load applied on the model footing is mostly carried by the individual soil particles and there is significantly less contribution to the frictional resistance from strength of bonds between the soil particles (Oh et al., 2009). In the current study, since the footing size is relatively large (i.e., 100 mm in diameter) compared to the median soil particle size (i.e., $D_{50} = 0.134$ mm), contribution from matric suction to soil shear strength is expected. By investigating the regularity in height, radius and shape of the surface bulging for each test, as well as the shape of the footing stress-settlement curves (i.e., whether there is a peak along the curve or not), the failure mode corresponding to each initial degree of saturation may be determined.

Stress-Settlement Curves for Soil Layers Improved with a Single Stone Column

This section focuses on the impact of the stone columns on the stress-settlement behavior for improved soil layers having different initial degrees of saturation. The loading details are the same as those explained in the first series of tests on the unimproved soil layers, and two groups of tests were performed. In the first group, the footing was subjected to loading until a settlement of 30 mm (i.e., normalized settlement of 0.3) was reached, after which the specimens were deconstructed to measure the deformed shapes of the stone column. In the second group, the footing was subjected loading until a settlement of 70 mm (i.e., normalized settlement of 0.7), which is assumed to fully mobilize the bearing capacity, was reached, and the specimens were then deconstructed. The relationships between applied stress and settlement of footing atop the unsaturated soil layers improved with a single stone column at different degrees of saturation from the second group of tests are shown in Figure 9. The bearing capacity of the soil

layers improved with a stone column follows the same trend with initial degree of saturation as the bearing capacity of the unimproved soil layers.

An issue of interest in this study is the determination of the deformations that occur in the stone column after the soil layer reaches its bearing capacity. To maintain the deformed shape of the stone column after completion of the test, gypsum slurry was poured into the stone column while trying not to affect or disturb its shape. After hardening of the slurry, the soil surrounding the stone column was carefully removed, and the depth of the bulging region and the dimensions of the deformed column were measured. For the tests conducted up to a settlement of 70 mm, because of the high compaction in the upper portion of the stone column materials, the gypsum could not permeate through the stones very well, and for some tests the column was cut along symmetry line to observe the deformed shape.

Photograph of a typical single stone column before loading is shown in Figure 10(a), and those after footing settlements of 30 and 70 mm are shown in Figure 10(b) and 10(c), respectively. A schematic shape of the deformed column is shown in Figure 10(d). Information about the deformations of the stone column at footing settlements of 30 and 70 mm are presented in Table 3. The least amount of bulging was observed in the test on the soil layer having an initial degree of saturation of 16%, for which the highest bearing capacity was also obtained. The largest bulging zones are also observed for the column installed in the soil layer at an initial degree of saturation of 90%, for which the lowest bearing capacity was also obtained. However, the dry soil layer is able to provide a greater resistance to deformation of the stone column than the soil layer with an initial degree of saturation of 90%.

At a footing settlement of 30 mm, stone column deformations were observed to occur up to a depth almost equal to 1/4 of the initial stone column length. This is approximately equivalent to 2 times the initial diameter of the stone column. At a footing settlement of 70 mm, the bulging zone in all the cases is such that deformations started from the soil surface and continued to a depth of approximately 1/3 of the initial column length. This is equivalent to about 3.5 to 4.0 times the initial stone column diameter. Generally, slight changes in these variables are noted with increasing initial degree of saturation.

ANALYSIS

Bearing Capacities of Unimproved and Improved Soil Layers

According to the results of loading on unimproved soil layers, the initial degree of saturation of the soil layer can alter the failure mode under the model shallow footing. In this section, the variation of the bearing capacity of unimproved and improved soil layers are presented. The tangent method was used to define the bearing capacity and failure for the curves with no peak for both the improved and unimproved soil layers with stone columns. The point of intersection of tangents to the two sections of the stress-settlement curve with larger and smaller slopes was determined, and the stress corresponding to this point was used as the bearing capacity (Vesic, 1963). However, for stress-settlement curves with an obvious peak, the peak stress was taken as the bearing capacity. The Variations in bearing capacity with the initial degree of saturation for both the improved and unimproved soil layers are shown in Figure 11. The improved soil layers have a greater bearing capacity than the unimproved soil layers, but the degree of saturation has a similar effect on the bearing capacity of both them. When the initial degree of saturation of the soil layer increases from 0 to 16%, the bearing capacity increases in

both the improved and unimproved soil layers. However, lower bearing capacities are observed for initial degrees of saturation greater than 16%, but smaller decreasing trend with the degree of saturation are observed in both series of experiments. These results indicate that the relationship between the bearing capacity and the initial degree of saturation is highly nonlinear, likely due to the change in the failure mode with the initial degree of saturation.

The bearing capacity measurements from the unimproved soil layers present an opportunity to evaluate the effective stress analyses of the bearing capacity in unsaturated soils, which permits an evaluation of whether the unsaturated conditions in the compacted soil layers follow logical trends expected from theory. Although this analysis does not consider the role of improvement with stone columns, it can be used together with the bearing improvement ratios presented later in the paper to predict the bearing capacity of unsaturated soil layers improved with stone columns.

Vahedifard and Robinson (2015) predicted the bearing capacity of unsaturated soils by incorporating the suction stress-based effective stress of Lu et al. (2010) into the general bearing capacity equation of Terzaghi (1943) through the total cohesion concept. A term referred to as total cohesion is introduced by adding the apparent cohesion (i.e., c_{app}) to the effective cohesion (i.e., $c_{total} = c_{app} + c'$). The total cohesion is then used in Terzaghi's bearing capacity equation to compute the ultimate bearing capacity of unsaturated soils. The apparent cohesion is defined as the shear strength mobilized by σ^s through the internal friction angle $c_{app} = -\sigma^s \tan\phi'$ (Lu et al., 2009). The bearing capacity equation of Vahedifard and Robinson (2015) is presented as follows:

$$q_{ult} = \{c' + (u_a - u_w)_b(1 - S_{e,\,AVR})\tan\phi' + [(u_a - u_w)S_e]_{AVR}\tan\phi'\}N_c\xi_c + q_0 N_q \xi_q + 0.5\gamma B N \quad (7)$$

where $(u_a - u_w)_b$ is the suction from the SWRC corresponding to the air-entry value (i.e., AEV), $S_{e,AVR}$ is the average effective saturation within the proximity of the stress bulb zone, i.e., 0 to 1.5B, below a shallow foundation (for the procedure employed in preparation of the soil in the experiments, there is an uniform profile of degree of saturation and matric suction beneath the footing, as a result the average matric suction and matric suction beneath the loading footing have got the same value), ξ_c, ξ_q, and ξ_γ are the shape factors defined using the equations of Vesić (1973), N_c, and N_q bearing capacity factors determined from the equations of Terzaghi (1943), and N_γ is a bearing capacity factor determined using the equation of Kumbhojkar (1993). The effective cohesion was assumed to be zero, and the friction angle ϕ'_m was modified to consider dilatancy effects, as follows:

$$\phi'_m = \phi' + \Psi \quad (8)$$

where Ψ is the dilatancy angle. It has been noticed that there is a good match between measured and computed bearing capacities when the effective internal friction angle, ϕ', is increased by 10 to 15% (Steensen-Bach et al., 1987). In this study the dilation angle was taken to be $0.1\phi'$. While the type of failure at degrees of saturations of 0% to 16% is likely of the general shear type, determination of the exact failure type for other degrees of saturation seems more challenging. Vertical stress-settlement curves for the footings on soil layers having these initial degrees of saturation exhibited no peak value, and the failure mode of the soil may be still in a transitional state that is closer to the local shear mode. The mode of failure of the soil influences the bearing capacity and shape factors used in calculations. Two different predicted capacities for the soil layers at degrees of saturation higher than 60% were considered. Values of the parameters used in the predicted bearing capacities for the unimproved soil layers are presented in Table 4. In the

predicted 1 series, it is assumed that the soil experiences local shear, whereas at the predicted 2 series, it is assumed that the soil layer experience a transitional behavior. The parameters used for the predicted 2 capacities are the average of the parameters of local and general shear failures. A comparison of the measured bearing capacity values for the unimproved soil layers with the predicted bearing capacity from the model of Vahedifard and Robinson (2015) is shown in Figure 12. A relatively reasonable match is observed between the predicted and the experimental values, especially in degrees of saturations in which the mode of failure of the soil is better recognized, with the greatest difference observed at a degree of saturation of 30% where a transitional behavior from general to local shear failure seems to occur.

Effect of Soil Bearing Capacity on Stone Column Behavior

The variations of maximum diameter of the stone column after bulging with the bearing capacity of the improved soil layers for footing settlements of 30 and 70 mm are shown in Figure 13. It can be inferred from this figure that bulging of the stone column is also directly related to the soil bearing capacity, indicating that both aspects of behavior are related to the shear strength of the unsaturated soil. This is consistent with the increase in effective stress and the higher confinement expected in soils that exhibit higher bearing capacities, leading to smaller deformations and bulging in these soils. Another interesting observation is that when the deformed column for the tests with a footing settlement of 70 mm was cut through its longitudinal section, an unclogged zone within the column near the soil-column interface was observed. In other words, there was no migration of soil particles into the pores of the column and, therefore, the influence of suction on the stone column particles is expected to be negligible.

Since the column is stiffer than the surrounding soil, distribution of the vertical stress beneath the footing and on the soil surface is non-uniform (Low et al., 1994; Indraratna et al., 2012). The difference in the stress distribution can be quantified using the stress concentration ratio, n_s, which is the ratio of the stress carried by stone column, σ_c, to the stress carried by the surrounding soil, σ_s, and is defined as:

$$n_s = \frac{\sigma_c}{\sigma_s} \tag{9}$$

The area of the soil replaced with the stone column material can be quantified using the Area Replacement Ratio, a_r, which is the ratio of the stone column area after construction (A_c) to the total area within the unit cell (A), such that $A = A_c + A_s$, in which A_s is the area of soil within the unit cell. The average applied stress over the tributary area, σ_t, can be quantified in terms of the Area Replacement Ratio, a_r, as follows:

$$\sigma_t = a_r\sigma_c + \sigma_s(1 - a_r) \tag{10}$$

In this case, σ_s and σ_c can be calculated as follows:

$$\sigma_s = \frac{\sigma_t}{1 + (n_s - 1)a_r} \tag{11}$$

$$\sigma_c = \frac{n_s\,\sigma_t}{1 + (n_s - 1)a_r} \tag{12}$$

Assuming that the cylindrical zone below the footing constitutes a unit cell, σ_s and σ_t can be defined as the stresses in the unimproved and improved soil layers, respectively. The stress in the stone column can then be calculated as follows:

$$\sigma_c = \frac{\sigma_t - (1 - a_r)\sigma_s}{a_r} \tag{13}$$

Variations of the stress concentration ratio (n_s) with normalized settlement for different initial degrees of saturation of the soil layers are shown in Figure 14, while variations of the bulging diameter of stone column versus the stress concentration factor (n_s) at different normalized settlement of the footing are shown in Figure 15. It can be noticed from Figure 15 that as the stress concentration ratio increases, the deformed diameter of the stone column also increases. There is a complex interaction among the unsaturated soil, column, and footing especially in small settlements. However, as shown in Figure 14, the curves with solid markers (corresponding to soil at higher degrees of saturations) are above those with hollow markers for which the degrees of saturation are lower. This is expected since soils with higher degrees of saturation are softer than those with lower degrees of saturation with typically higher bearing capacities and, therefore, columns installed in soils closer to saturated state will provide greater contribution in resisting the applied loads.

Bearing Improvement Ratio for Improvement of Unsaturated Soils with a Single Stone Column

The improvement of soil layers using stone columns was observed to lead to a clear increase in the bearing capacity of a surface footing. To quantify this improvement, the bearing capacity of the unimproved, unsaturated soil can be estimated using the model in the previous section, and can then be multiplied by a bearing improvement ratio, defined as follows:

$$n_i = \frac{q_{improved}}{q_{unimproved}} \quad (14)$$

where $q_{unimproved}$ is the bearing capacity of the unimproved soil layer and $q_{improved}$ is the bearing capacity of the improved soil layers. Variations of the bearing improvement ratio (n_i) versus displacement of footing at different initial degrees of saturation of soil layers are shown in Figure

16, and variations of the bearing improvement ratio (n_i) at failure as well as the variation of average stress concentration ratio (n_s) for different degrees of saturation are depicted in Figure 17. Some variations in the bearing improvement ratio with the initial degree of saturation are shown in Figure 16, and an overall average value of approximately 2 is observed. On the other hand, Figure 17 shows that the initial degree of saturation of the soil affects the stress-deformation response of the stone column, as quantified by the stress concentration factor, but it may not have a major effect on the bearing improvement ratio. However the columns installed in wetter soils (with degrees of saturation of 60 and 90%) provide greater contribution in improvement of the soil. More specifically, for the soil at degrees of saturation of 16 and 90%, values of improvement ratio are 1.55 and 2.10, respectively at normalized displacements of approximately 5%, which occur under typical service loads.

The findings presented in this study are based on loading of a single stone column. In practice, stone columns are usually used in groups, and the mechanism of load transfer within groups of stone columns is somewhat different from that in a single stone column. If stone columns are sufficiently close to each other it is anticipated that the bulging potential of one stone column will be restricted by that of the adjacent columns and that, as a result, in the center of the group, the load will be transmitted to greater depths (Wood et al., 2000). For an infinitely large group of stone columns subjected to a uniform loading applied over the whole improved area, interior stone columns will behave similarly and each of them may be considered as a unit cell. Due to symmetry of load and geometry, lateral deformations cannot occur across the boundaries of the unit cell, and the shear stresses on the outside boundaries of the unit cell must be zero (Barksdale and Bachus, 1983). Except near the edges of the loaded area, the behavior of

all stone column-soil units in such cases is the same and thus, only one stone column-soil unit needs to be analyzed (Balaam et al. 1978). Following these assumptions, a uniform loading applied over the top area of the unit cell must remain within the unit cell. There are several researchers that have employed the concept of unit cell in modelling the behavior of stone columns in a large group (e.g., Ambily and Gandhi, 2007; Gniel and Bouazza, 2009; and Castro et al., 2014). When the column area alone is loaded, failure typically occurs due to stone column bulging. Past studies have shown that results of single stone column tests with an entire unit cell area loaded compare well with the group test results and, hence, the single stone column behavior studied within a unit cell concept can simulate the field behavior for an interior column when a group of stone columns are simultaneously loaded (Ambily and Gandhi, 2007).

A number of approaches have been adopted in the past to numerically model and analyze stone column behavior. Some researchers used finite element analyses to evaluate the influence of stiffness of stone columns on their load-deformation behavior (e.g., Balaam et al., 1977). A 2D/axisymmetric finite element parametric study has also been proposed to provide a prediction of settlements of granular columns by some other researchers (e.g., Sexton et al., 2014). However, the effects of characteristics of the surrounding unsaturated soils on the settlements and deformations have not been considered in these studies. An important consideration in numerical modeling of stone columns is the consideration of dilatancy of the column granular material. It is very difficult to actually measure the dilatancy angle of such material, especially in the field (Herle et al., 2008). Castro (2014) carried out numerical modelling of stone columns beneath a rigid footing in which, he used a reasonable estimation of soil dilatancy based on in-situ soil properties. Results of a recent numerical study carried out on the behavior of stone

columns installed in unsaturated soil showed that such analyses can also be used to verify and supplement model testing results. This study indicates that realistic prediction of the effects of degree of saturation on the behavior of stone columns in unsaturated soils may be obtained if a proper SWRC and variations of soil properties with degree of saturation are used in the numerical modeling (Imam and Fotowwat, 2018).

Conclusion

This paper presents the results of stress-deformation behavior of 1g physical model tests on unsaturated soil layers improved with a single stone column. Results indicate that changes in the initial degree of saturation of the soil layer can have a major effect on the bearing capacity of the soil layer, the soil failure mode during loading of a surface footing, and the deformation interaction responses of the soil layer and the embedded stone column. The changes in bearing capacity with initial degree of saturation were observed to align with estimates from an effective stress model, if changes in the failure mode from general shear failure to local shear failure are considered. Deformations of the improved soil exhibited a close relationship with its bearing capacity, indicating that both aspects of behavior of the improved soil are related to the shear strength of the unsaturated soil. Minimum and maximum dimensions of the bulging zone were observed in the soil layers with the highest and lowest bearing capacities, respectively. The bulging zone in the columns started from the soil surface and continued to a depth of approximately 1/4 and 1/3 of the initial length of the stone column, after footing normalized settlements of 0.3 and 0.7 mm, respectively. These amounts are approximately equivalent to 2 and 4 times the initial diameter of the stone column, respectively. An approach to predict the impact of unsaturated conditions on the bearing

capacity of unsaturated soils improved using stone columns was proposed, where a bearing improvement ratio is multiplied by the bearing capacity estimated using an effective stress model. Trends of variation of the initial degree of saturation with the stress concentration ratio are provided in order to quantify the effects of this variable on the bulging diameter of the stone column.

References

Aboshi, H., Ichimoto, E., Enoki, M. and Harada, K., 1979. The compozer—a method to improve characteristics of soft clays by inclusion of large diameter sand columns, Proc., Int. Conf. on Soil Reinforcement., ENPC, pp. 211-216.

Ambily, A. and Gandhi, S.R., 2007. Behavior of stone columns based on experimental and FEM analysis. Journal of Geotechnical and Geoenvironmental Engineering, 133(4): 405-415.

Ayadat, T. and Hanna, A., 2005. Encapsulated stone columns as a soil improvement technique for collapsible soil. Proceedings of the Institution of Civil Engineers-Ground Improvement, 9(4): 137-147.

Babu, M.D., Nayak, S. and Shivashankar, R., 2013. A critical review of construction, analysis and behaviour of stone columns. Geotechnical and Geological Engineering, 31(1): 1-22.

Baker, R. and Frydman, S., 2009. Unsaturated soil mechanics: Critical review of physical foundations. Engineering Geology, 106(1): 26-39.

Barksdale, R. and Bachus, R., 1983. Design and Construction of Stone Columns, Federal Highway Administration. Report FHWA/RD-83/027.

Bishop, A.W., 1959. The principle of effective stress. Teknisk ukeblad, I Samarbeide Med Teknikk, Oslo, Norway, 106(39): 859-863.

Balaam, N., Brown, P., and Poulos, H. 1977. Settlement analysis of soft clays reinforced with granular piles. 5th Southeast Asian Conference on Soil Engineering, Bangkok, Thailand.

Black, J., Sivakumar, V. and McKinley, J., 2007. Performance of clay samples reinforced with vertical granular columns. Canadian Geotechnical Journal, 44(1): 89-95.

Broms, B.B., 1965. Effect of degree of saturation on bearing capacity of flexible pavements. Highway Research Record, 71: 1-14.

Bouazza, A., Zornberg, J.G., McCartney, J.S. and Nahlawi, H., 2006. Significance of unsaturated behaviour of geotextiles in earthen structures. Australian Geomechanics, 41(3): 133-142.

Bouazza, A., Zornberg, J., McCartney, J.S. and Singh, R.M., 2013. Unsaturated geotechnics applied to geoenvironmental engineering problems involving geosynthetics. Engineering Geology, 165: 143-153.

Brooks, R. H., and Corey, A. T., 1964. Hydraulic properties of porous media. Colorado State University, Hydrology Paper No. 3, March.

Cerato, A.B. and Lutenegger, A.J. 2007. Scale effects of shallow foundation bearing capacity on granular material. Journal of Geotechnical and Geoenvironmental Engineering. 133(10): 1192-1202.

Clayton, W. S., 1996. Relative permeability-saturation-capillary head relationships for air sparging in soils. Ph.D. Dissertation, Colorado School of Mines, Golden, CO.

Castro, J., 2014. Numerical modelling of stone columns beneath a rigid footing. Computers and Geotechnics, 60: 77-87.

Castro, J., Karstunen, M. and Sivasithamparam, N., 2014. Influence of stone column installation on settlement reduction. Computers and Geotechnics, 59: 87-97.

Costa, Y.D., Cintra, J.C. and Zornberg, J.G., 2003. Influence of matric suction on the results of plate load tests performed on a lateritic soil deposit. Geotechnical Testing Journal, 26(2): 219-227.

Das, A.K. and Deb, K., 2016. Response of cylindrical storage tank foundation resting on tensionless stone column-improved soil. International Journal of Geomechanics, 17(1): 04016035.

Dash, S.K. and Bora, M.C., 2013. Influence of geosynthetic encasement on the performance of stone columns floating in soft clay. Canadian Geotechnical Journal, 50(7): 754-765.

Deb, K., Samadhiya, N.K. and Namdeo, J.B., 2011. Laboratory model studies on unreinforced and geogrid-reinforced sand bed over stone column-improved soft clay. Geotextiles and Geomembranes, 29(2): 190-196.

Fredlund, D.G., 2014. Foreword: The Emergence of Unsaturated Soil Mechanics. NRC Research Press, Ottawa.

Fredlund, D.G. and Rahardjo, H., 1993. Soil Mechanics for Unsaturated Soils. John Wiley & Sons, 517 pp.

Fredlund, D.G., Xing, A., Fredlund, M.D. and Barbour, S., 1996. The relationship of the unsaturated soil shear to the soil-water characteristic curve. Canadian Geotechnical Journal, 33(3): 440-448.

Gens, A., Sánchez, M. and Sheng, D., 2006. On constitutive modelling of unsaturated soils. Acta Geotechnica, 1(3): 137-147.

Gniel, J. and Bouazza, A., 2009. Improvement of soft soils using geogrid encased stone columns. Geotextiles and Geomembranes, 27(3): 167-175.

Gniel, J. and Bouazza, A., 2010. Construction of geogrid encased stone columns: A new proposal based on laboratory testing. Geotextiles and Geomembranes, 28(1): 108-118.

Greenwood, D., 1970. 2. Mechanical improvement of soils below ground surface. Ground Engineering. Inst Civil Engineers Proc. London, UK., pp. 11-22.

Herle, I., Wehr, J., and Arnold, M., 2008. Soil improvement with vibrated stone columns: influence of pressure level and relative density on friction angle. Proceedings of the 2nd International Conference on the Geotechnics of Soft Soils, Glasgow.

Hossain, M.A. and Yin, J.-H., 2014. Dilatancy and strength of an unsaturated soil-cement interface in direct shear tests. International Journal of Geomechanics, 15(5): 04014081.

Hughes, J. and Withers, N., 1974a. Reinforcing of soft cohesive soils with stone columns. Ground Engineering, 7(3): 42-49.

Iai, S., 1989, “Similitude for shaking table tests on soil-structure-fluid models in 1g gravitational fields.” Soils Found. 29(1): 105–118.

Imam, R., Fotowwat, A.R., 2018. Numerical modelling of stone columns in unsaturated silty sand. 7th International Conference on Unsaturated Soils (UNSAT2018). C.W.W. Ng, A.K. Leung, A.C.F. Chiu, C. Zhou, eds. The Hong Kong University of Science and Technology. 191-196. 6 pg.

Imam, R., Vaseghi M., S., and McCartney, J.S. (2018). Shear strength of unsaturated sand at different relative densities. 7th International Conference on Unsaturated Soils

(UNSAT2018). C.W.W. Ng, A.K. Leung, A.C.F. Chiu, C. Zhou, eds. The Hong Kong University of Science and Technology. 191-196.

Indraratna, B., Basack, S. and Rujikiatkamjorn, C., 2012. Numerical solution of stone column–improved soft soil considering arching, clogging, and smear effects. Journal of Geotechnical and Geoenvironmental Engineering, 139(3): 377-394.

Khalili, N., Khabbaz, M. and Valliappan, S., 2000. An effective stress based numerical model for hydro-mechanical analysis in unsaturated porous media. Computational Mechanics, 26(2): 174-184.

Kumbhojkar, A., 1993. Numerical evaluation of Terzaghi's Nγ. Journal of Geotechnical Engineering, 119(3): 598-607.

Lau, C.K. and Bolton, M.D. 2011. The bearing capacity of footings on granular soils. II: Experimental evidence. Géotechnique. 61(8): 639-650.

Low, B., Tang, S. and Choa, V., 1994. Arching in piled embankments. Journal of Geotechnical Engineering, 120(11): 1917-1938.

Lu, N., 2008. Is matric suction a stress variable? Journal of Geotechnical and Geoenvironmental Engineering, 134(7): 899-905.

Lu, N., Godt, J.W. and Wu, D.T., 2010. A closed-form equation for effective stress in unsaturated soil. Water Resources Research, 46(5): 14.

Lu, N., Kim, T.-H., Sture, S. and Likos, W.J., 2009. Tensile strength of unsaturated sand. Journal of Engineering Mechanics, 135(12): 1410-1419.

Madhav, M. and Vitkar, P., 1978. Strip footing on weak clay stabilized with a granular trench or pile. Canadian Geotechnical Journal, 15(4): 605-609.

McCartney, J.S., Kuhn, J.A., Zornberg, J.G., 2005. Geosynthetic drainage layers in contact with unsaturated soils. Proceedings 16th International Conference of Soil Mechanics and Geotechnical Engineering, Osaka, Japan, September 12–17, pp. 2301–2305.

McQueen, I.S. and Miller, R.F., 1974. Approximating soil moisture characteristics from limited data: empirical evidence and tentative model. Water Resources Research, 10(3): 521-527.

Miller, G. and Muraleetharan, K., 1998. In situ testing in unsaturated soil, Proceedings of the Second International Conference on Unsaturated Soils, Beijing, China, pp. 416-421.

Mohamed, F. and Vanapalli, S., 2006. Laboratory investigations for the measurement of the bearing capacity of an unsaturated coarse-grained soil, Proceedings of the 59th Canadian Geotechnical Conference, Vancouver, BC, pp. 1-4.

Muir Wood, D., Hu, W. and Nash, D., 2000. Group effects in stone column foundations: model tests. Geotechnique, 50(6): 689-698.

Oh, S., Lu, N., Kim, Y.K., Lee, S.J. and Lee, S.R., 2011. Relationship between the soil-water characteristic curve and the suction stress characteristic curve: Experimental evidence from residual soils. Journal of Geotechnical and Geoenvironmental Engineering, 138(1): 47-57.

Oh, W.T. and Vanapalli, S.K., 2011. Modelling the applied vertical stress and settlement relationship of shallow foundations in saturated and unsaturated sands. Canadian Geotechnical Journal, 48(3): 425-438.

Oh, W.T. and Vanapalli, S.K., 2013. Scale effect of plate load tests in unsaturated soils. Int. J. Geomater, 4(2): 585-594.

Oh, W.T., Vanapalli, S.K. and Puppala, A.J., 2009. Semi-empirical model for the prediction of modulus of elasticity for unsaturated soils. Canadian Geotechnical Journal, 46(8): 903-914.

Oloo, S.Y., Fredlund, D. and Gan, J.K., 1997. Bearing capacity of unpaved roads. Canadian Geotechnical Journal, 34(3): 398-407.

Palmer, L., 1948. Field Loading Tests for the Evaluation of the Wheel-Load Capacities of Airport Pavements, Symposium on Load Tests of Bearing Capacity of Soils. ASTM International, pp. 9-30.

Schnaid, F., Consoli, N., Cudmani, R. and Militistsky, J., 1995. Load-settlement response of shallow foundations in structured unsaturated soils, Proceedings of the First International Conference of Unsaturated Soils, Paris, France, pp. 999-1004.

Shahu, J. and Reddy, Y., 2011. Clayey soil reinforced with stone column group: model tests and analyses. Journal of Geotechnical and Geoenvironmental Engineering, 137(12): 1265-1274.

Sexton, B. G., McCabe, B. A., and Castro, J., 2014. Appraising stone column settlement prediction methods using finite element analyses. Acta Geotechnica, 9(6), 993-1011.

Shivashankar, R., Babu, M.D., Nayak, S. and Manjunath, R., 2010. Stone columns with vertical circumferential nails: laboratory model study. Geotechnical and Geological Engineering, 28(5): 695-706.

Steensen-Bach, J., Foged, N. and Steenfelt, J., 1987. Capillary induced stresses—fact or fiction?, European Conference on Soil Mechanics and Foundation Engineering. 9, pp. 83-89.

Tang, Y., Taiebat, H.A. and Russell, A.R., 2016. Bearing capacity of shallow foundations in unsaturated soil considering hydraulic hysteresis and three drainage conditions. International Journal of Geomechanics, 17(6): 040161421-0401614213.

Terzaghi, K., 1943. Theoretical Soil Mechanics. John Wiley and Sons, New York, NY, USA.

Vahedifard, F. and Robinson, J.D., 2015. Unified method for estimating the ultimate bearing capacity of shallow foundations in variably saturated soils under steady flow. Journal of Geotechnical and Geoenvironmental Engineering, 142(4): 04015095.

van Genuchten, M.T., 1980. A closed-form equation for predicting the hydraulic conductivity of unsaturated soils. Soil Science Society of America Journal, 44(5): 892-898.

Vanapalli, S.K. and Mohamed, F.M., 2013. Bearing capacity and settlement of footings in unsaturated sands. Int. J. of GEOMATE, 5(1): 595-604.

Vesic, A.B., 1963. Bearing capacity of deep foundations in sand. Highway research record (39): 112-153.

Vesić, A.S., 1973. Analysis of Ultimate Loads of Shallow Foundations. Journal of the Soil Mechanics and Foundations Division, 99(1): 45-73.

637 Table 1- Geotechnical properties of the silty sand and stone.

Property	silty sand	Stone Column Material
Specific gravity, G_s	2.64	2.69
Maximum dry unit weight, $\gamma_{d(max)}$ (kN/ m^3)	15.5	15.9
Minimum void ratio, e_{min}	0.68	0.67
Minimum dry unit weight, $\gamma_{d(min)}$ (kN/ m^3)	13.6	13.3
Maximum void ratio, e_{max}	0.90	0.98
Coefficient of curvature, C_z	0.85	1.50
Coefficient of uniformity, C_u	1.99	6.00
Fines content ($<$ 0.075 mm, %)	7.0	0
Target relative density (%)	40	60
Target dry unit weight, γ_d (kN/ m^3)	14.3	14.7
Target void ratio, e	0.81	0.80
Drained friction angle at the target void ratio, ϕ' (°)	32.6	38.6
Air- entry value suction, $(u_a - u_w)_b$ (kPa)	1.67	-
Residual degree of saturation, S_{res} (%)	0	-
van Genuchten (1980) SWRC fitting parameter, α_{vG} (kPa^{-1})	0.27	-
van Genuchten (1980) SWRC fitting parameter, n_{vG}	2.14	-

638
639
640
641
642

Table 2- Synthesis of the failure envelopes for the seven series of direct shear tests on specimens with different initial degrees of saturation.

Degree of saturation, S_r (%)	Gravimetric water content, w (%)	Friction angle, ϕ' (°)	Apparent cohesion, c_{app} (kPa)	Coefficient of determination, R^2
0	0	32.6	0.00	0.9976
4	1	32.6	1.21	0.9986
16	5	32.6	2.05	0.9989
30	9	32.6	1.91	0.9999
60	18	32.6	1.71	0.9987
90	28	32.6	0.89	0.9942
100	30.7	32.6	0.00	0.9917

Table 3- Dimensions of the deformed stone column for tests with various initial degrees of saturation of the soil layer at settlements of 30 and 70 mm.

S_r (%)	h_{max}		d_{max}		h/d		d_{max}/d	
	d= 30 mm	d= 70 mm	d= 30 mm	d= 70 mm	d= 30 mm	d= 70 mm	d= 30 mm	d= 70 mm
0	62	120	75	107	1.84	3.80	1.50	2.14
4	62	130	75	110	1.84	4.00	1.50	2.20
16	67	120	70	100	1.94	3.80	1.40	2.00
30	65	110	70	105	1.90	3.60	1.40	2.10
60	60	120	77	110	1.80	3.80	1.54	2.20
90	60	120	79	110	1.80	3.80	1.58	2.20

Table 4- Values of parameters used in the analysis of different bearing capacity predictions (Vahedifard and Robinson, 2015) for the unimproved soil layers.

S_r (%)	Type of failure	Description	Effective cohesion, c' (kPa)	$\phi'(°)$	$\phi'_m(°)$	N_c	N_q	N_γ	ξ_c	ξ_γ
0% to 30%	General Shear		0	32.6	35.8	58	44	49.7	1.8	0.6
60% to 90%	Local Shear	Predicted 1 (Local)		23.1	25.7	27	14	6	1.5	0.6
	Average of local and General	Predicted 2 (Transitional)		-	-	42	29	33	1.69	0.6

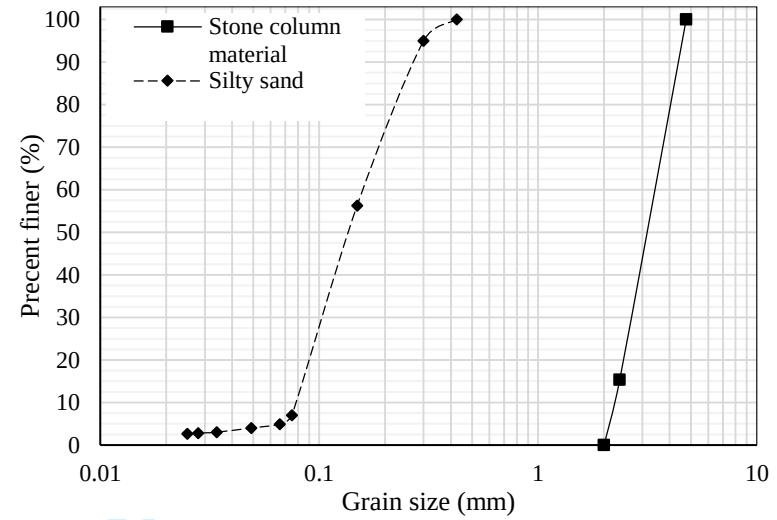

(a)

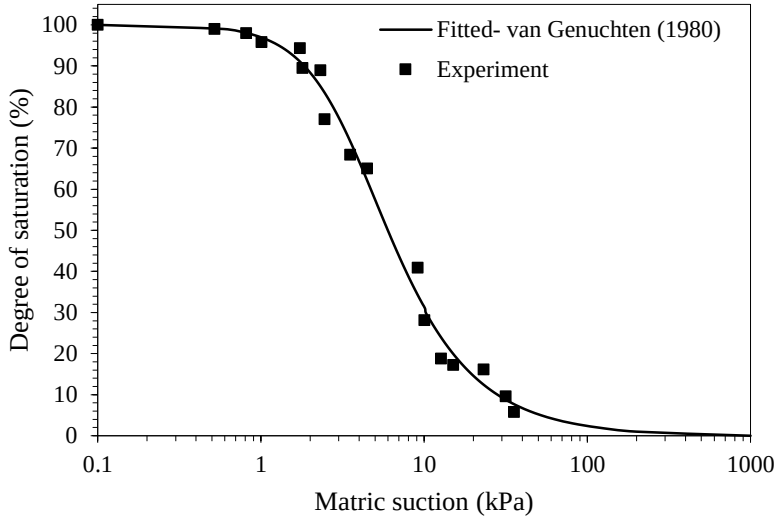

(b)

Figure 1- (a) Grain size distributions for the silty sand and stone column material; (b) SWRC of the silty sand at a relative density of 40%.

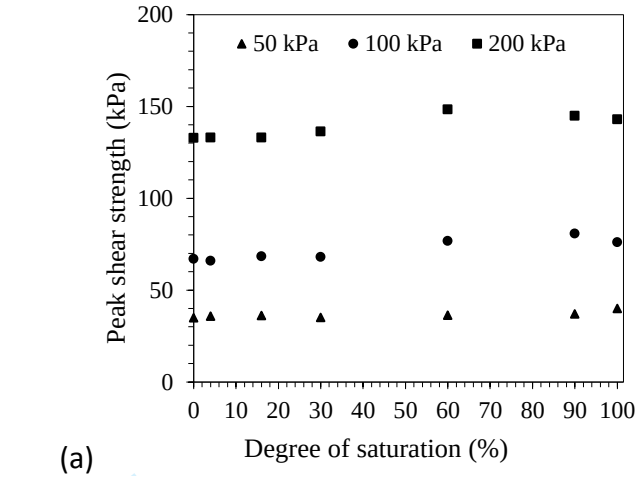

(a)

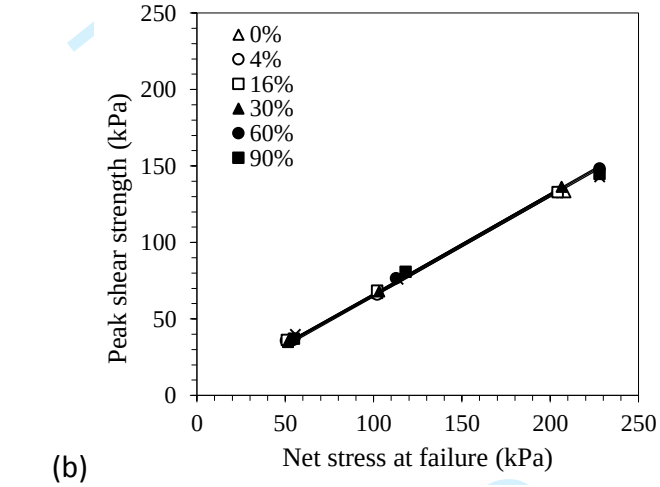

(b)

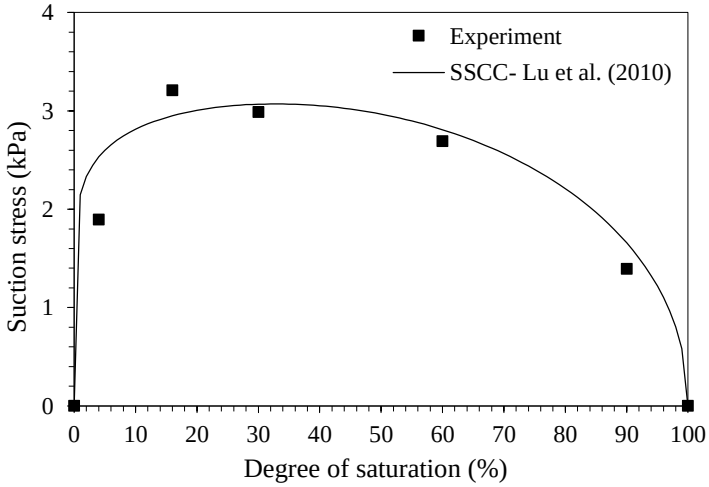

(c)

Figure 2- Shear strength of the unsaturated silty sand: (a) Variation of peak shear strength with initial degree of saturation for different initial vertical total stresses; (b) Failure envelopes in terms of net vertical stress for different initial degrees of saturation; (c) Variation of suction stress with the initial degree of saturation.

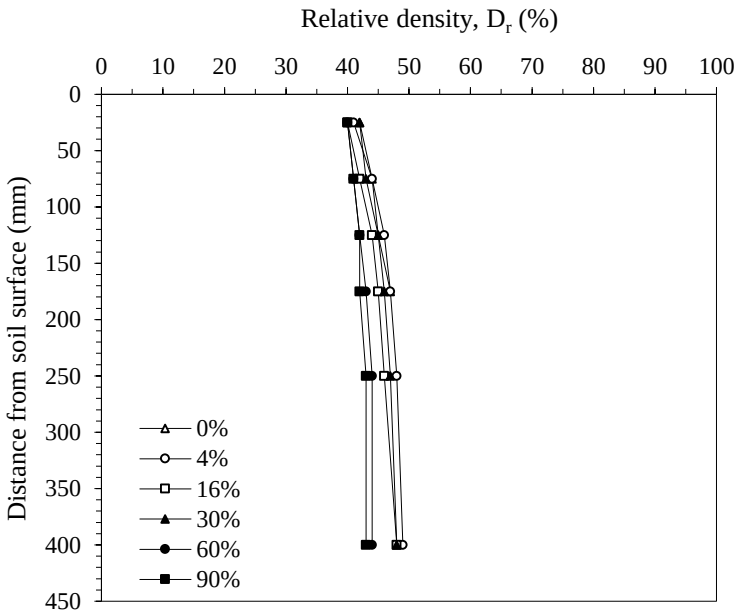

Figure 3- Relative density variations with depth after installing unimproved soil layers having various initial degrees of saturation.

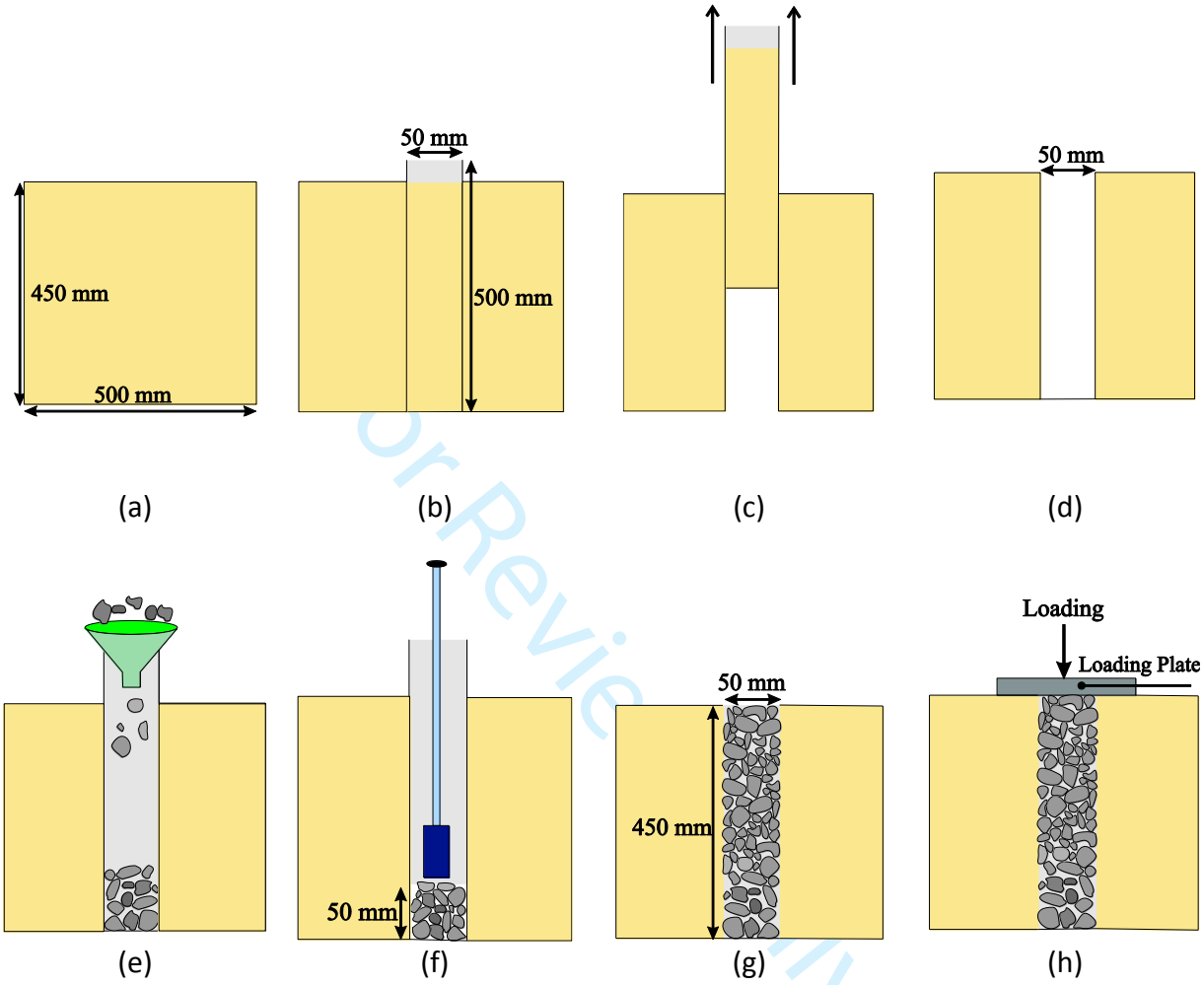

Figure 4- Procedures for stone column installation and evaluation: (a) Construction of the soil layer at a desired degree of saturation; (b) pushing an open-ended tube into the center of the soil layer; (c) extracting the soil inside the tube; (d) finishing the inner wall of the hole; (e) re-inserting the tube inside the hole and pouring stones into the hole; (f) compacting the stones to the finished height of 50 mm and diameter of 50 mm; (g) completion of the column to the final height of 450 mm and diameter of 50 mm and keeping the system for 7 days; (h) loading of a shallow footing on the soil surface 7 days after construction.

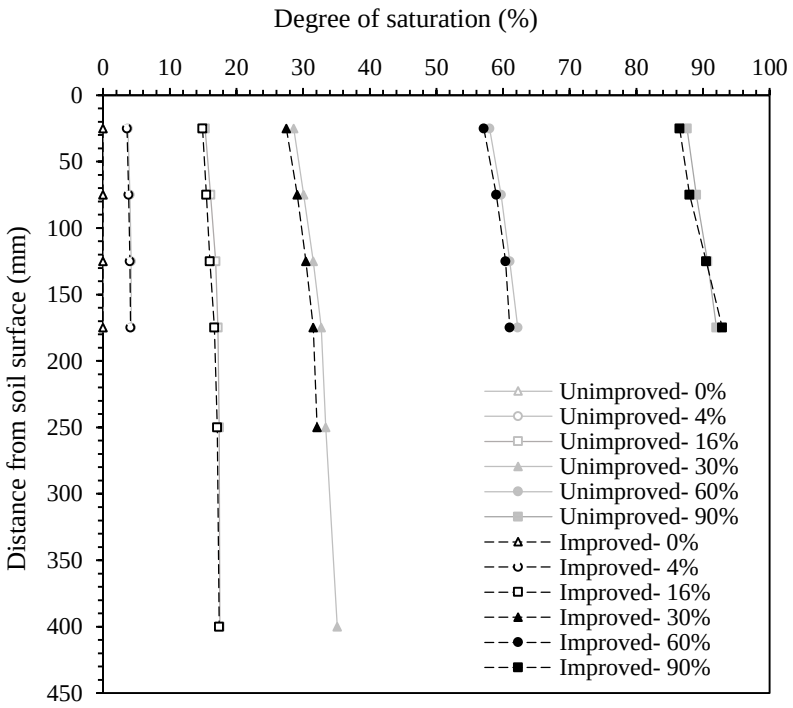

Figure 5- Profiles of initial (pre-loading) degrees of saturation of unimproved and improved soil layers corresponding to different initial average degrees of saturation.

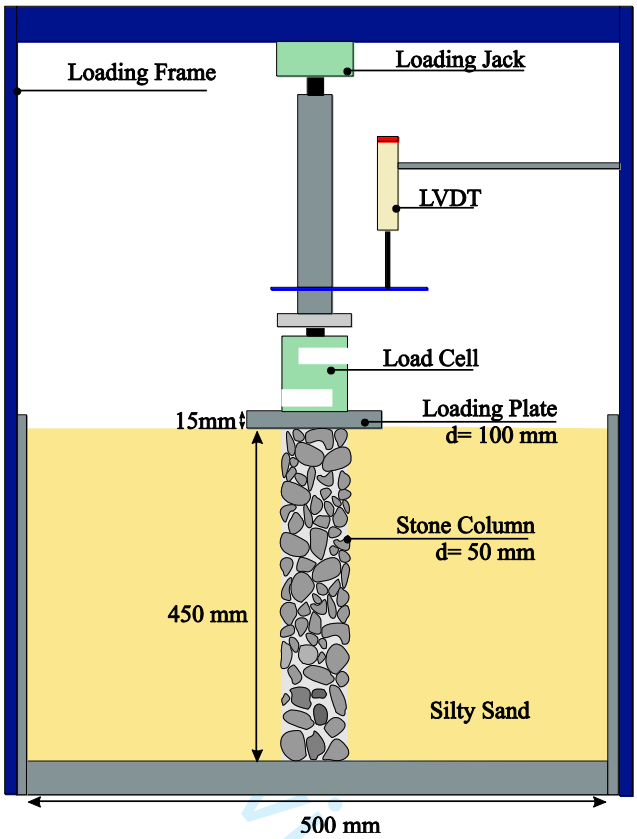

Figure 6- Details of the experimental setup for characterization of the axial loading response of soil layers treated with stone columns.

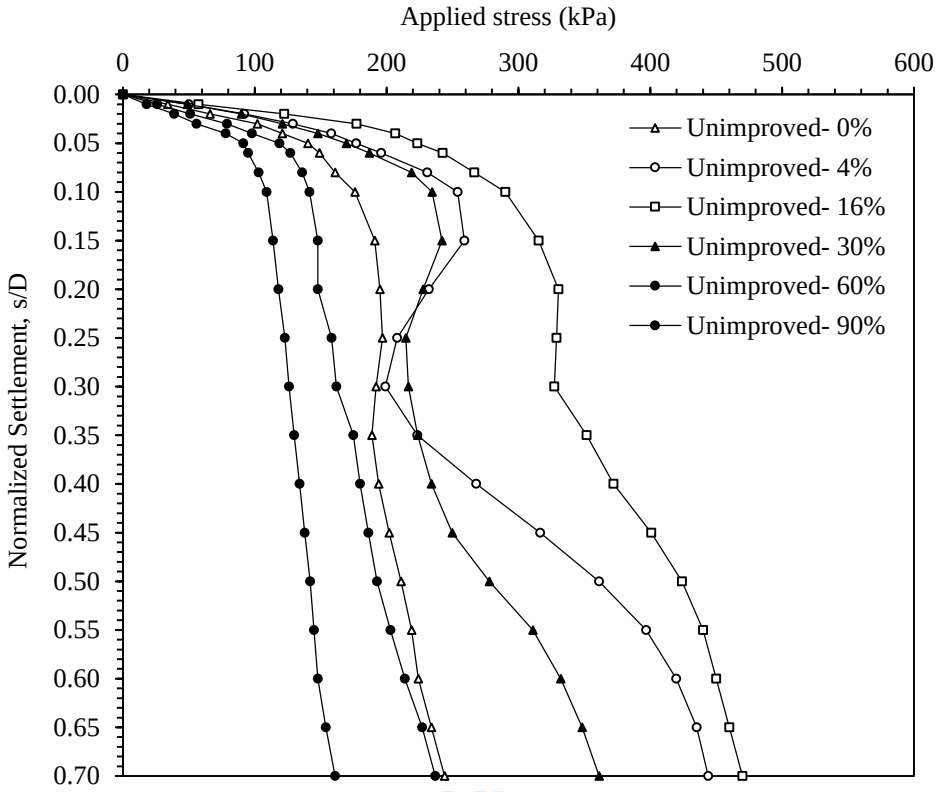

Figure 7- Relationships between the applied footing stresses versus settlement for unimproved soil layers compacted to different initial degrees of saturation.

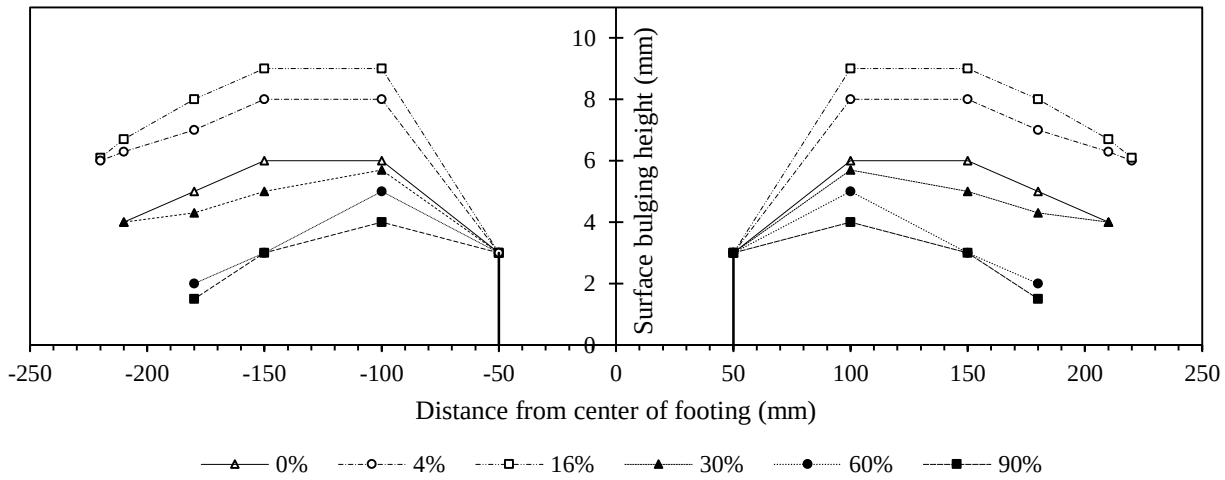

Figure 8- The shape of surface bulging for the unimproved soil layers at different initial degrees of saturation at a vertical footing settlement of 30 mm (i.e., s/D = 0.3).

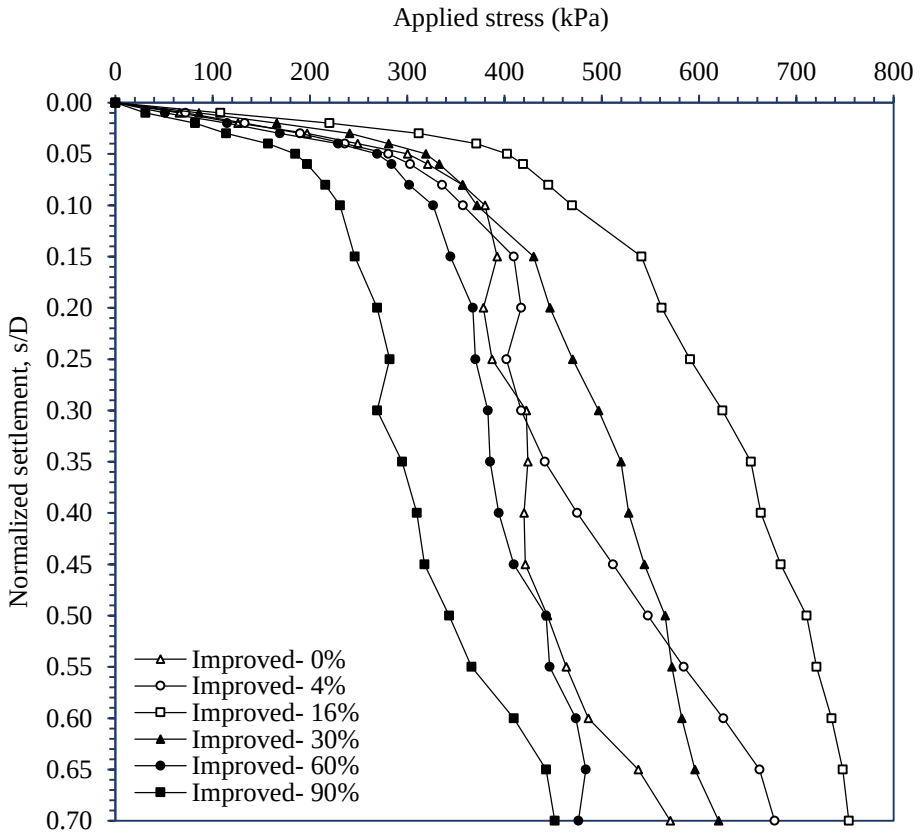

Figure 9- Relationships between the applied stress and settlement curves for the improved soil layers having different initial degrees of saturation

(a) (b) (c) (d)

Figure 10- (a) Initial stone column shape; (b) Stone column shape after a footing settlement of 30 mm; (c) stone column shape after a footing settlement of 70 mm; (d) Schematic of a typical deformed stone column.

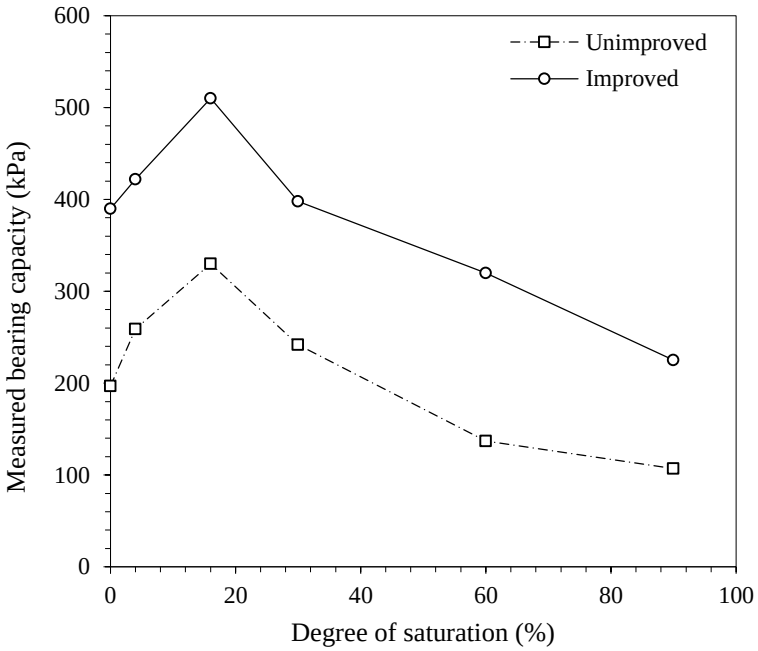

Figure 11- Variations in bearing capacity with the initial degree of saturation of the unimproved and unimproved soil layers.

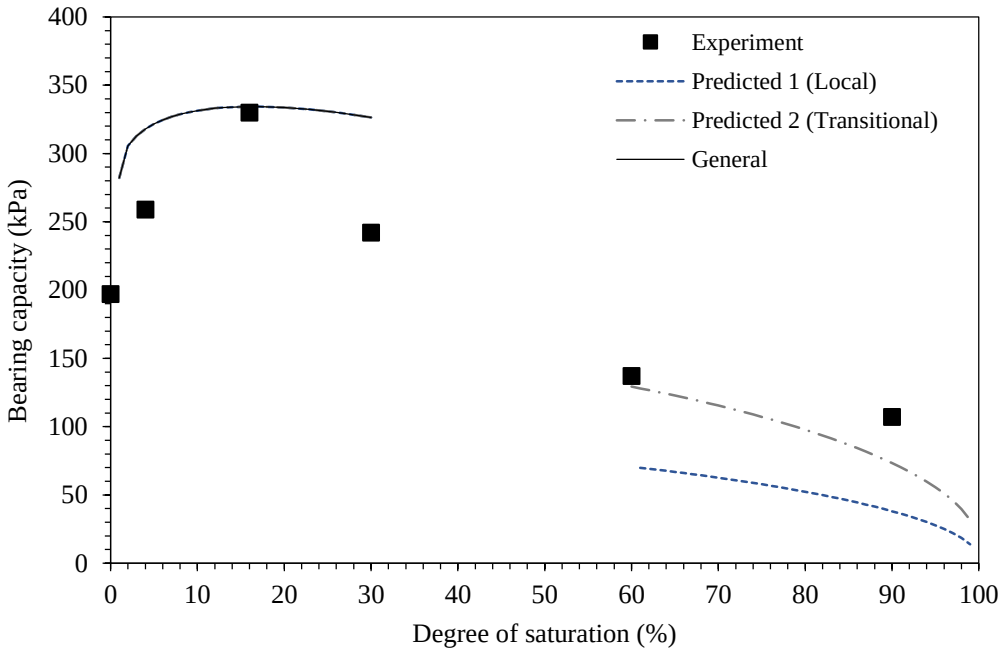

Figure 12- Comparison of experimentally measured and predicted bearing capacity for the unimproved soil layers (Note: General failure for initial degrees of saturation ranging from 0 to 30%, and local failure for initial degrees of saturation ranging from 60 to 90%).

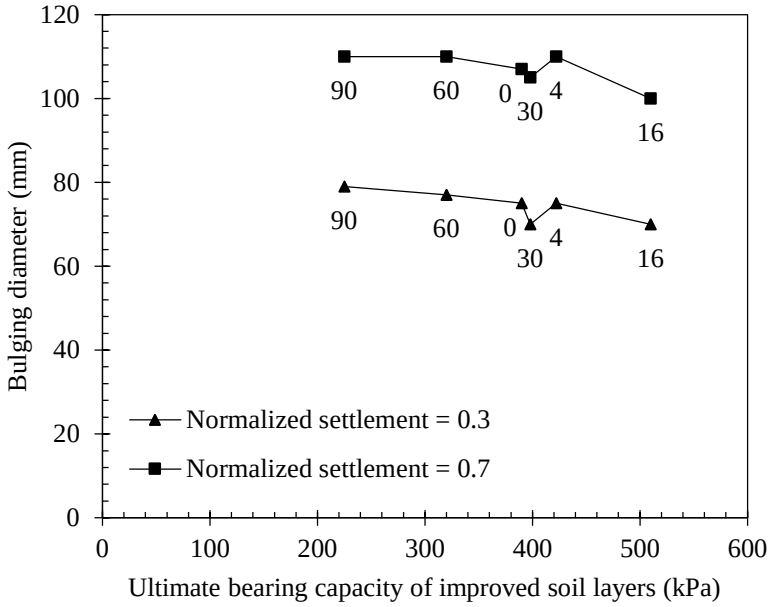

Figure 13- Variations of the maximum bulging of the stone column versus the bearing capacity of the improved soil layers (Note initial degrees of saturation of the soil layers are shown next to the data points).

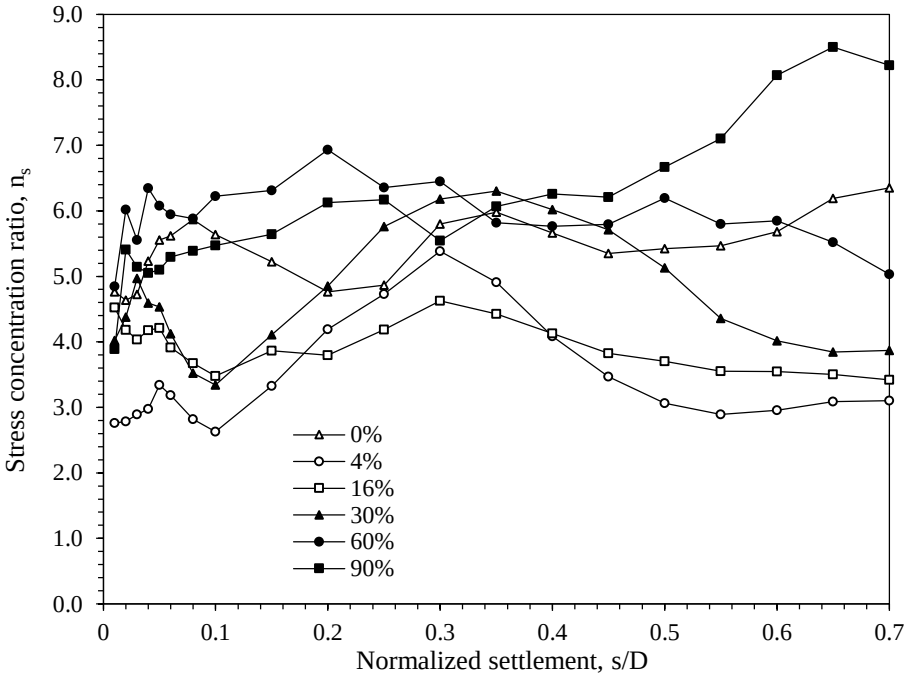

Figure 14- Variations of the stress concentration factor (n_s) versus footing settlement for improved soil layers having different initial degrees of saturation.

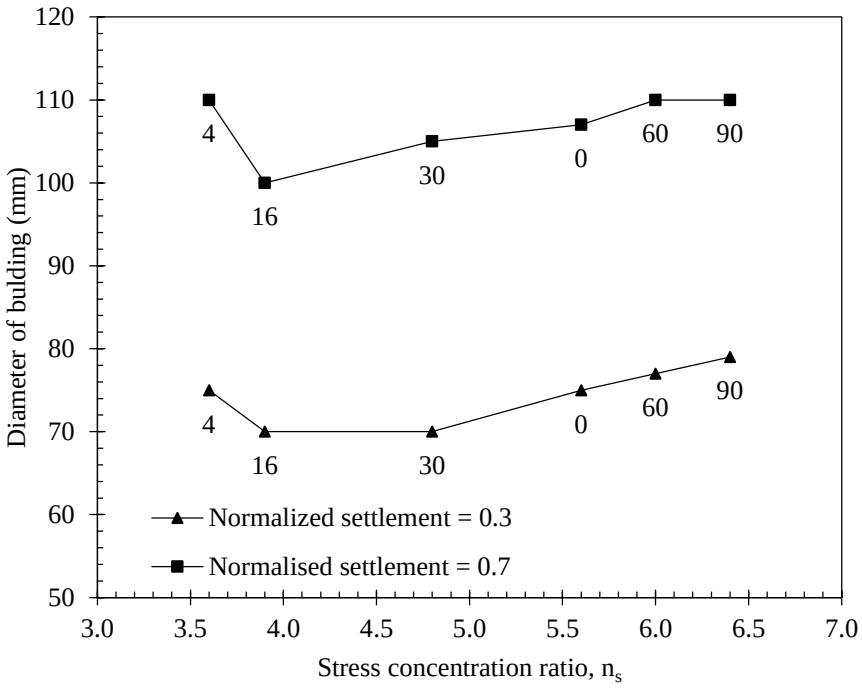

Figure 15- Variations of the diameter of bulging of the stone columns versus the stress concentration factor (n_s) at different footing settlements (Note initial degrees of saturation of the soil layers are shown next to the data points).

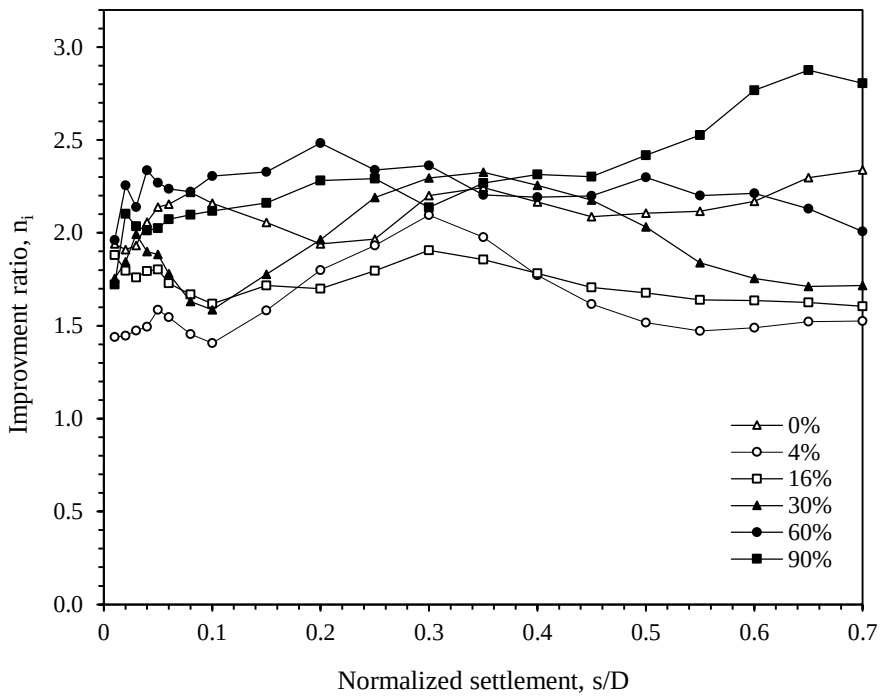

Figure 16- Variations of the bearing improvement ratio (n_i) versus footing settlement for soil layers having different initial degrees of saturation.

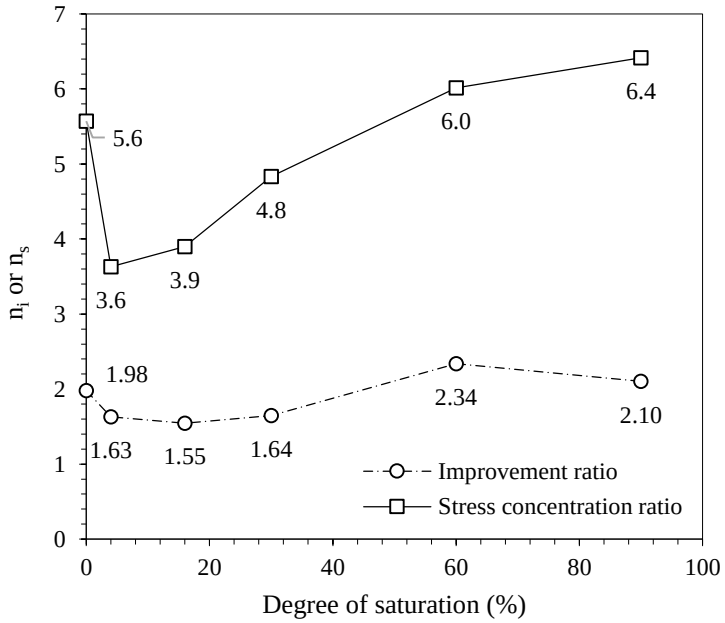

Figure 17- Variations of n_i and n_s for soil layers with different initial degrees of saturation.